

AD-A194 731

SOME EXPERIMENTS WITH UNDERWATER ACOUSTIC RETURNS FROM  
CYLINDERS RELATIVE TO OBJECT IDENTIFICATION FOR AUV  
OPERATION(U) NAVAL POSTGRADUATE SCHOOL MONTEREY CA  
M A FARREN MAR 88

1/1

UNCLASSIFIED

P/G 17/1

NL

END  
DATE  
FILMED  
8 8-8



1-C

2-8

2-5

3-15

2-2

3-5

2-0

4-0

1-8

1-5



1-1



1-25

1-4

1-6

AD-A194 731

2

# NAVAL POSTGRADUATE SCHOOL Monterey, California



## THESIS

**SOME EXPERIMENTS WITH UNDERWATER  
ACOUSTIC RETURNS FROM CYLINDERS  
RELATIVE TO OBJECT IDENTIFICATION  
FOR AUV OPERATION**

by

Maureen A. Farren

March 1988

Thesis Advisor:

Anthony J. Healey

Approved for public release; distribution is unlimited.

DTIC  
ELECTE  
JUL 05 1988

E

D

## REPORT DOCUMENTATION PAGE

1a. REPORT SECURITY CLASSIFICATION <b>UNCLASSIFIED</b>		1b. RESTRICTIVE MARKINGS	
2a. SECURITY CLASSIFICATION AUTHORITY		3. DISTRIBUTION/AVAILABILITY OF REPORT Approved for public release: distribution is unlimited	
2b. DECLASSIFICATION/DOWNGRADING SCHEDULE		5. MONITORING ORGANIZATION REPORT NUMBER(S)	
4. PERFORMING ORGANIZATION REPORT NUMBER(S)		7a. NAME OF MONITORING ORGANIZATION Naval Postgraduate School	
6a. NAME OF PERFORMING ORGANIZATION Naval Postgraduate School	6b. OFFICE SYMBOL (If applicable) CODE 69HY	7b. ADDRESS (City, State, and ZIP Code) Monterey, California 93943-5000	
8a. NAME OF FUNDING SPONSORING ORGANIZATION		9. PROCUREMENT INSTRUMENT IDENTIFICATION NUMBER	
8b. OFFICE SYMBOL (If applicable)		10. SOURCE OF FUNDING NUMBERS	
8c. ADDRESS (City, State, and ZIP Code)		PROGRAM ELEMENT NO	PROJECT NO
		TASK NO	WORK UNIT ACCESSION NO
11. TITLE (Include Security Classification) Some Experiments with Underwater Acoustic Returns from Cylinders Relative to Object Identification for AUV Operation			
12. PERSONAL AUTHOR(S) Farren, Maureen A.			
13a. TYPE OF REPORT Master's Thesis	13b. TIME COVERED FROM TO	14. DATE OF REPORT (Year Month Day) 1988, March	15. PAGE COUNT 43
16. SUPPLEMENTARY NOTATION The views expressed in this thesis are those of the author and do not reflect the official policy or position of the DOD or the U.S. Government.			
17. COSAT CODES		18. SUBJECT TERMS (Continue on reverse if necessary and identify by block number)	
FIELD	GROUP	SUB-GROUP	
		AUV Object Identification, Underwater Acoustic Imaging, for Intelligent Control System	
19. ABSTRACT (Continue on reverse if necessary and identify by block number) Object identification and avoidance by an autonomous underwater vehicle requires that a knowledge-based, intelligent control system have some way to quantify sonar returns from an object for comparison with stored data on simple shapes. One measurement of an insonified object is its target strength, which is dependent on geometrical shape and surface properties. This thesis examines various aspects of target strength for two geometrically similar, open-ended cylinders with different expected surface properties. Experimental data was obtained in an anechoic underwater chamber using two acoustic transducers where position of the cylindrical object was varied relative to the transducer's locations. Target strength estimates, as well as propagation time delay of the insonifying signal, were studied. The experimental results were compared to the calculated values of a fully insonified, finite cylinder.			
20. DISTRIBUTION/AVAILABILITY OF ABSTRACT <input checked="" type="checkbox"/> UNCLASSIFIED/UNLIMITED <input type="checkbox"/> SAME AS RPT <input type="checkbox"/> DTIC USERS		21. ABSTRACT SECURITY CLASSIFICATION Unclassified	
22a. NAME OF RESPONSIBLE INDIVIDUAL Prof. A.J. Healey		22b. TELEPHONE (Include Area Code) (408) 646-2586	22c. OFFICE SYMBOL Code 69HY

Approved for public release; distribution is unlimited.

**Some Experiments With Underwater Acoustic Returns From  
Cylinders Relative to Object Identification for AUV Operation**

by

Maureen A. Farren  
Lieutenant, United States Navy  
B.S., University of Southern California, 1980

Submitted in partial fulfillment of the  
requirements for the degree of

MASTER OF SCIENCE IN MECHANICAL ENGINEERING


from the

NAVAL POSTGRADUATE SCHOOL  
March 1988

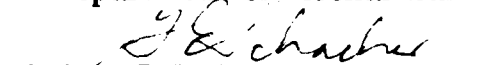
Author:

  
Maureen A. Farren

Approved by:

  
Anthony J. Healey, Thesis Advisor

  
Anthony J. Healey, Chairman,  
Department of Mechanical Engineering

  
Gordon E. Schacher, Dean of  
Science and Engineering

## ABSTRACT

Object identification and avoidance by an autonomous underwater vehicle requires that a knowledge-based, intelligent control system have some way to quantify sonar returns from an object for comparison with stored data on simple shapes. One measurement of an insonified object is its target strength, which is dependent on geometrical shape and surface properties. This thesis examines various aspects of target strength for two geometrically similar, open-ended cylinders with different expected surface properties. Experimental data was obtained in an anechoic underwater chamber using two acoustic transducers where position of the cylindrical object was varied relative to the transducer's locations. Target strength estimates, as well as propagation time delay of the insonifying signal, were studied. The experimental results were compared to the calculated values of a fully insonified, finite cylinder.

Accession For	
DTIC TAB	<input checked="" type="checkbox"/>
DTIC TAB	<input type="checkbox"/>
Unannounced	<input type="checkbox"/>
Justification	
By	
Distribution/	
Availability Codes	
Avail and/or	
Dist	Special
A-1	



## TABLE OF CONTENTS

<b>I. INTRODUCTION .....</b>	<b>1</b>
<b>II. BACKGROUND .....</b>	<b>3</b>
<b>III. EXPERIMENTAL SET-UP.....</b>	<b>6</b>
A. GENERAL .....	6
B. EXPERIMENTAL APPARATUS.....	6
C. DETERMINATION OF TARGET STRENGTH.....	12
D. SOURCE LEVEL VERIFICATION.....	14
<b>IV. RESULTS.....</b>	<b>19</b>
A. GENERAL .....	19
B. COMPARISON WITH ANALYTICALLY DERIVED TARGET STRENGTH ESTIMATES .....	32
C. LIMITATIONS DUE TO NOISE.....	34
D. CONCLUSIONS.....	34
E. RECOMMENDATIONS .....	35
<b>LIST OF REFERENCES.....</b>	<b>36</b>
<b>INITIAL DISTRIBUTION LIST.....</b>	<b>37</b>

## **I. INTRODUCTION**

The United States Navy has had an interest in unmanned, untethered, and fully autonomous vehicles for more than two decades. In recent years, interest has been focused on the long-range autonomous vehicle (LRAV), whose prospective missions include survey, interdiction, information gathering, and ocean engineering [Ref. 1]. The potential for LRAVs to execute forward area strategy has not been overlooked, nor has the requirement for extreme reliability in both mission hardware and software of the LRAV guidance and control system [Ref. 2]. One of the most critical subsystems would involve the obstacle-avoidance sensor and processor.

It is essential that the presence and nature of obstacles be sensed within a matter of seconds. The required LRAV maneuvers are different for encounters with mooring cables or piles, rocks or low lying objects, or impassable objects such as a breakwater. [Ref. 2]

While there have been a great many technological advances in the area of high-resolution imaging, such as side-scan sonar, infrared imaging, and low-light-level optics, most of these developments were designed to provide information for human processing [Ref. 3]. An imaging system for "intelligent control systems" must be designed to provide workable information that will allow the system to perceive its environment where little or no *a priori* information exists. This requires that the signal received by the sensors be quantifiable so that a knowledge-based system has the ability to reliably categorize the information and make decisions accordingly. One characteristic of a



target is its target strength, which is based on target geometry, material properties, and the insonification frequency. This thesis has investigated some aspects of target strength for cylinders with respect to differences in reflecting surfaces and spatial relation to the receiver.

## **II. BACKGROUND**

Work in object avoidance has been carried out with land-based robots using optical and infrared systems as well as with acoustics [Ref. 4]. While the latter systems have the advantage of good bearing resolution, they are very range limited in water, especially in the turbid and murky water that accounts for most of the in-shore waters and harbors as well as deep ocean soft-sediment bottoms. There has been a good deal of success in using transducers on land for mapping an area where multiple sensor readings are modelled as probability profiles and projected onto a map to represent empty or occupied spaces [Ref. 4]. The environment was modelled in a two-dimensional plane with regular geometric features, which is inadequate for representing a free-swimming vehicle with six degrees of freedom in an irregular environment such as the ocean floor [Ref. 5]. Additionally, the system gives little information on what the obstacle is, only showing whether it is present.

One type of sonar system which produces high-resolution images is the side-scan sonar. While developed for mapping horizontal sea floors, the technology shows promise for use on vertical and sloped surfaces and, in some cases, large curved surfaces [Ref. 6]. There are, however, several limitations which place constraints on the development of a system suitable for an AUV. To obtain accurate information from the side-scan sonar, a stable platform which can be moved rela-

tive to the surface in a controlled manner with constant speed, heading, altitude, and low rates of yaw is required. In addition, little progress has been reported in signal-processing algorithms for side-scan sonar with respect to image analysis and pattern recognition. [Ref. 7]

The most successful body of work associated with sonar imaging for AUVs relies on a knowledge-based process for the intelligent control system whereby sensor input is evaluated and compared to known information or models so that appropriate action can be taken by the system [Ref. 8]. In the case of a sonar signal, the echo received must be classified as either:

1. the primary echo reflected from an object
2. multi-path reflections which correspond to objects which do not exist
3. noise from other acoustic sources, surface reflection, or reverberation.

Real objects exhibit temporal correlation in their global axis position and produce a set of measurement features (size, shape, speed, etc.) within boundaries which can be defined *a priori* by a training set. Real objects thus identified will have a limited range of shapes because of poor spatial resolution of sonar. [Ref. 9]

Stewart [Ref. 5] has designed a 3-D underwater model for sonar mapping. He starts with the basic sonar equation and uses probabilistic methods to account for non-ideal sensors. In the basic equation, target strength is replaced by a more general term of scattering strength. Uniform scattering in all directions is assumed so that only the spatial distribution of scattering strength is modeled.

Actual target strength is determined primarily by object size, shape, and the frequency of the incident sound. Little is known about the frequency dependence of the target strength for most targets [Ref. 10]. The target strength is a function of its sonar cross-section  $\sigma$ , which can be determined analogously to radar cross-sections. High-frequency approximations for several basic target shapes partially insonified by a sonar beam have been published [Ref. 11]. If the knowledge-based system will be required to evaluate and categorize target shapes, additional knowledge with regard to target strength of objects must evolve.

### **III. EXPERIMENTAL SET-UP**

#### **A. GENERAL**

This chapter describes the experimental configuration used to obtain the data for this thesis. To investigate the influence of object distance, orientation, and relative position, a ranging system and two cylindrical "targets" were installed in an underwater anechoic chamber. The set-up, preliminary results, and target strength evaluations are given here.

#### **B. EXPERIMENTAL APPARATUS**

A ranging system was designed using an Atlantic Research LC-10 transducer as a noise source and an EDO/Western model 6600 omnidirectional transducer as the receiver. The EDO was chosen due to its availability and its relatively flat frequency response from 0 to 300 kHz. The two hydrophones were mounted on plastic tubing 2.0 cm apart and 71.0 cm below the surface of the water. The experiment was carried out in an anechoic water tank of the dimensions illustrated in Figure 1.

A Hewlett-Packard 3314A function generator was used to produce a 200 kHz burst with a 2.30 msec sweep of amplitude 6.0 volts. The signal was sent through a Hewlett-Packard 476A power amplifier, then to the source transducer. The output was monitored on a Kikusui model COS5060A oscilloscope.

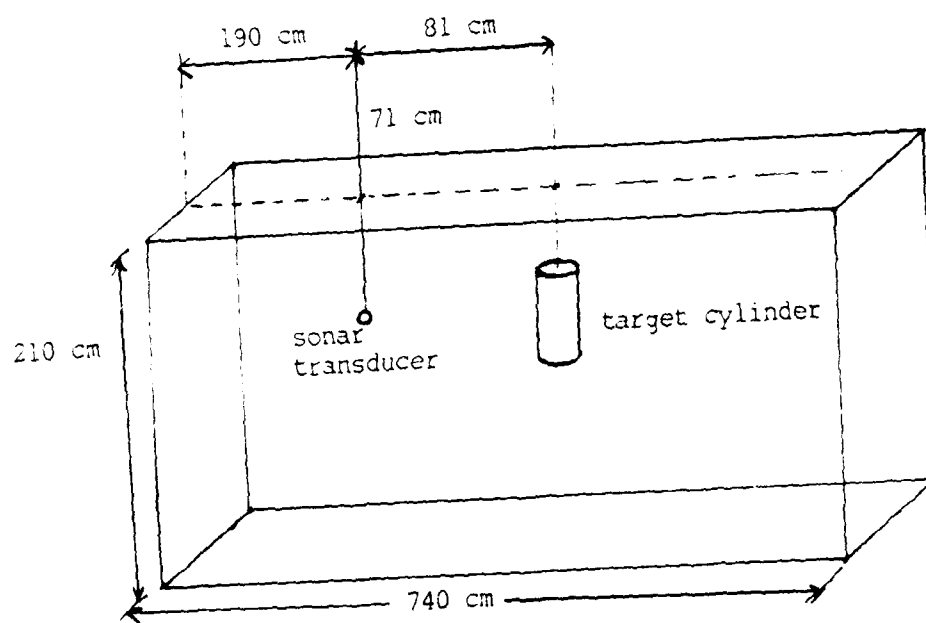


Figure 1. Side View of Tank

The return signal from the EDO transducer was amplified through a Tektronix TM-501 power module using 100 gain and a 10 kHz-1 Mhz bandwidth, then to the second channel of the oscilloscope. Figure 2 shows a diagram of the experimental equipment configuration used.

The targets used to generate an echo consisted of two similarly sized hollow, open-ended cylinders—one of aluminum and the other of PVC plastic. Dimensions were 37.0 cm in length and 17.0 cm OD. Two configurations were used: The cylinders were either suspended vertically or horizontally in the water. Depth and position relative to the transducer were then varied, and data on the time delay and amplitude of the return signal were then recorded for all configurations. Figures 3 and 4 illustrate the geometry of the transducers and targets.

Distances to targets were computed by multiplying the time delay of the return by the speed of sound ( $c$ ) in water. A water temperature of 20.0° C was recorded and the speed of sound of the water was computed using the following empirical formula [Ref. 10]:

$$c = 1449.05 + 45.7 T - 5.21 T^2 + 0.23 T^3 \\ + (1.333 - 0.126 T + 0.009 T^2) (S - 35) \quad (1)$$

where

$S$  = salinity in PPT ( $S = 0$ )

$T$  = 20° C/10

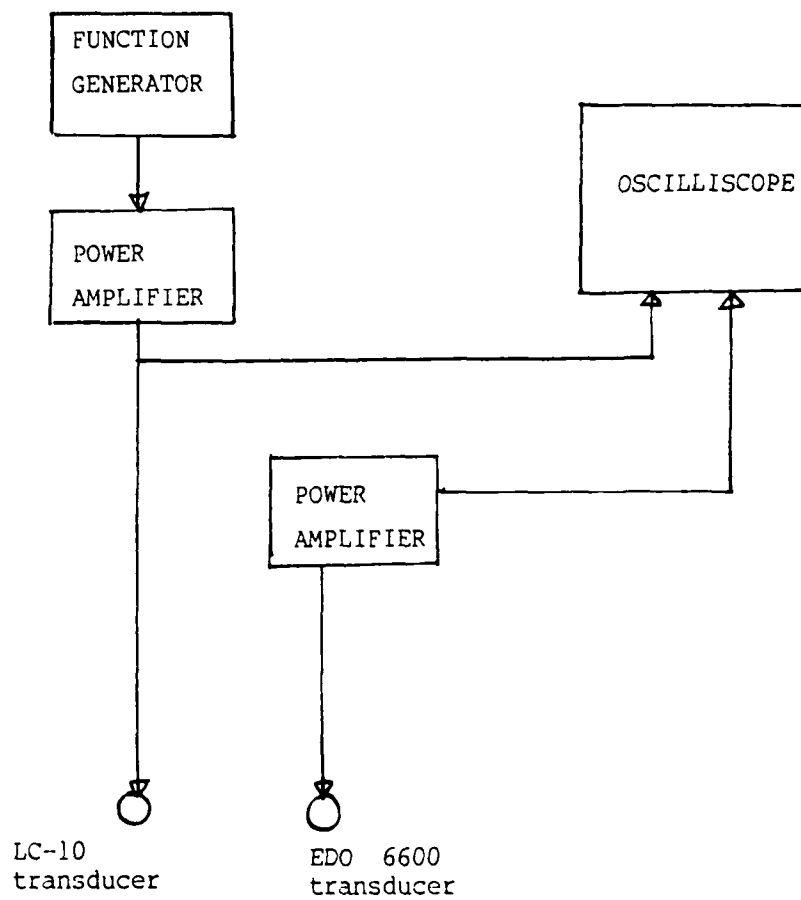
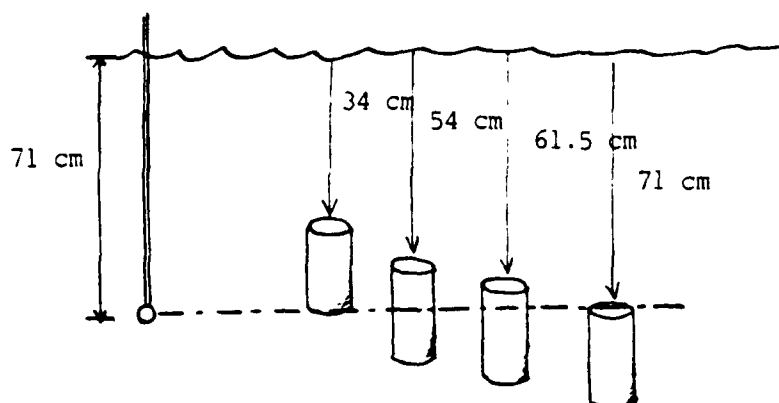
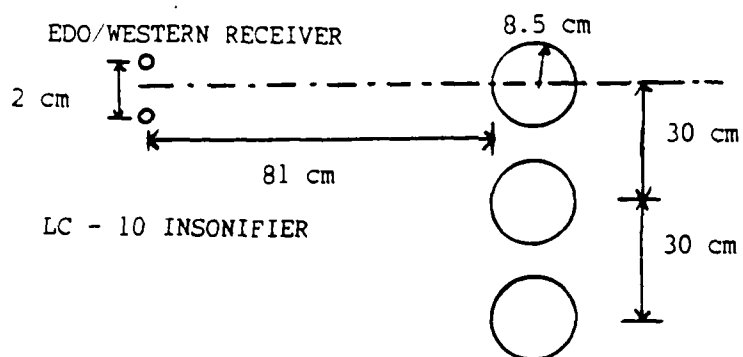


**Figure 2. Acoustic System**



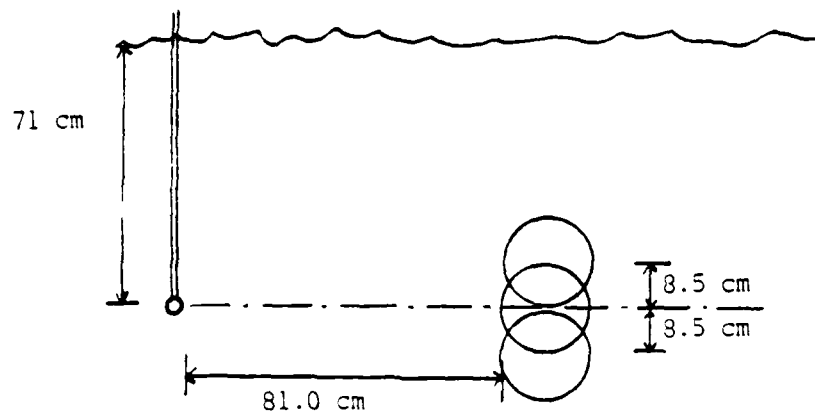


Side view showing spatial relationship for depth variation. (Note: distance in longitudinal direction was not changed.)

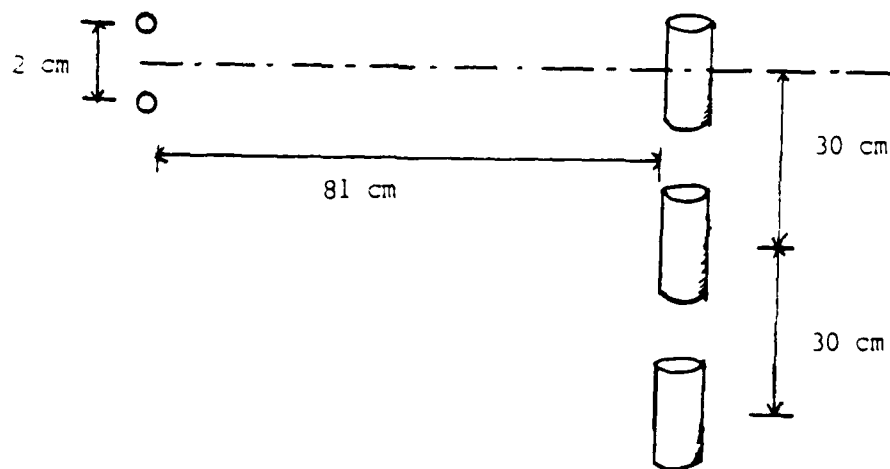


Overhead view

Figure 3. Vertical Cylinder Set-Up



Side view showing depth variation.



Overhead view

Figure 4. Horizontal Cylinder Set-Up

The calculated value for  $c$  used in this experiment was  $c = 1482.46$  m/s.

### C. DETERMINATION OF TARGET STRENGTH

The determining equation for this experiment was the sonar equation for active sonar:

$$EL = SL - TL - TL' - TS \quad (2)$$

where

EL = echo level at receiver (dB)

SL = source level (dB)

TL = TL' = transmission loss through water (dB)

TS = target strength (dB)

Figure 5 graphically depicts the relationship of the terms used.

A general model for transmission loss of the source level was based on the model for loss due to spherical spreading in a fluid, which is given by [Ref. 10]:

$$TL = AR + 20 \log \left( \frac{R}{R_0} \right) \quad (3)$$

where  $A$  is the sound absorption coefficient in DB/M. By convention, the  $\log R$  term is normally nondimensionalized by  $R_0 = 1.0$  M, but due to the short distances measured in this experiment (80-120 cm), this term proved unsuitable for our analysis. By definition,  $TL = 0$  at the

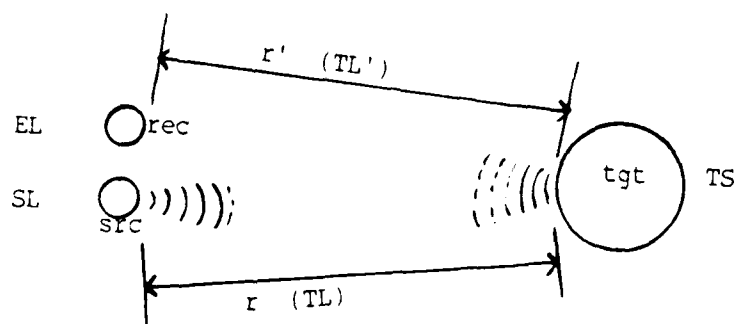


Figure 5. Model for Active Sonar Equation

source, therefore the  $R_0$  chosen for this experiment was the radius of the source transducer;  $R_0 = .635$  cm, the AR term in the basic equation is so small at  $R = R_0$  (less than  $5 \times 10^{-4}$  dB/cm) that it can effectively be considered zero for the purposes of this experiment.

The sound absorption coefficient (A) for water can be closely approximated from the relationship  $A = C(F)^2$ , where F is the frequency in Hz and the coefficient (C) can be found from the empirical formula [Ref. 10]:

$$C = 4.76 \times 10^{-13} (1.0 - 4.0 \times 10^{-2} T + 5.9 \times 10^{-4} T^2) \times (1.0 - 3.8 \times 10^{-4} P_0) \quad (4)$$

where

$$T = 20^\circ \text{ C}$$

$$P_0 = 1.0 \text{ ATM}$$

C was found to be  $2.0746 \times 10^{-13}$  and  $A = 8.298 \times 10^{-5}$  dB/cm.

The final transmission loss equation used for all calculations was:

$$TL = (8.29825 \times 10^{-5} \text{ dB/cm}) (R) + 20 \log (R/0.635 \text{ cm}) \quad (5)$$

#### **D. SOURCE LEVEL VERIFICATION**

To verify the validity of this equation for future calculations, the receiving transducer was placed at roughly the depths and distances that the targets would later be placed. The amplitude of the received signals was recorded and then compared with the calculated values.

As can be seen from Figure 6, the actual values generally fell within  $\pm 1$  dB of the calculated values, with the largest deviation of  $\pm 2$  dB. The amplitude data from this initial test was also graphed versus depth and horizontal offset, with respect to the source. As can be seen in Figure 7, when any given depth is held constant, and the horizontal displacement is varied, the apparent level at the target site drops off 2 to 3 dB as one approaches the outer limits of 60.0 cm offset from the center. Additionally, when offset is held constant and depth is varied, the site level drops off 3 to 5 dB at the upper and lower extremes of depth, which corresponds to 37.0 cm above and below the source transponder level (Figure 8). Both graphs reveal that the farther away a target is from the perpendicular line relative to the source transducer, the less accurate the model for transmission loss and, consequently, target strength.

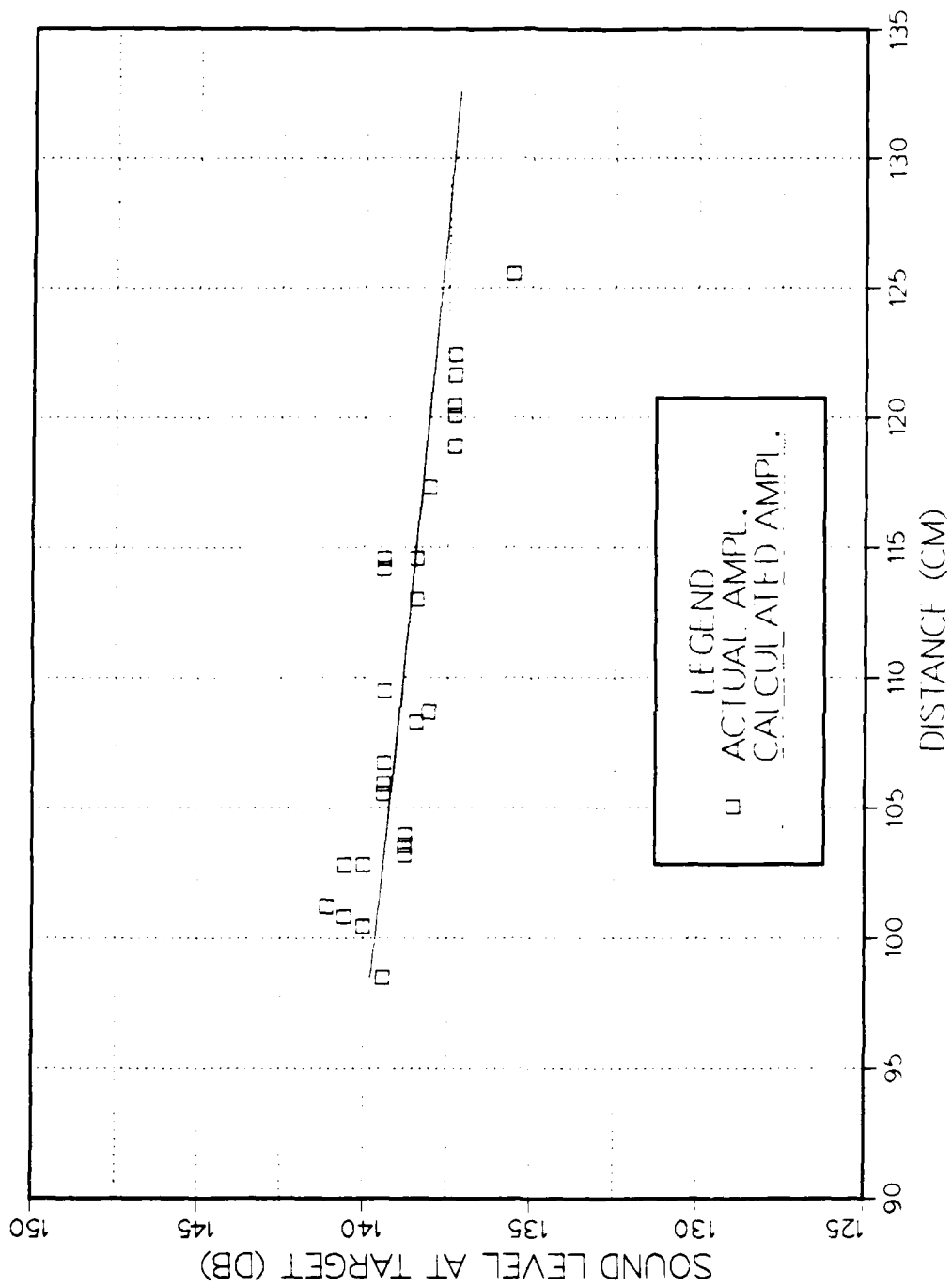


Figure 6. Direct Path Transmission Loss

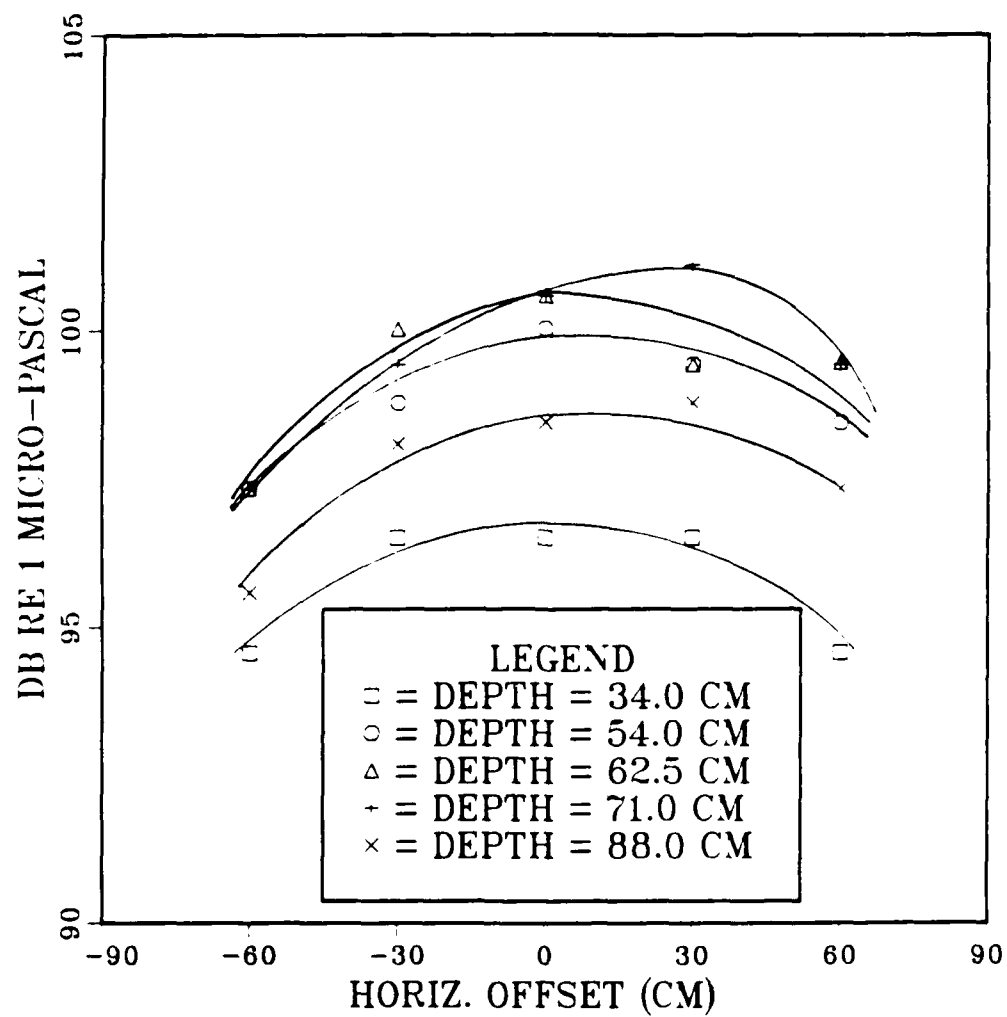


Figure 7. Sound Level at Target Site



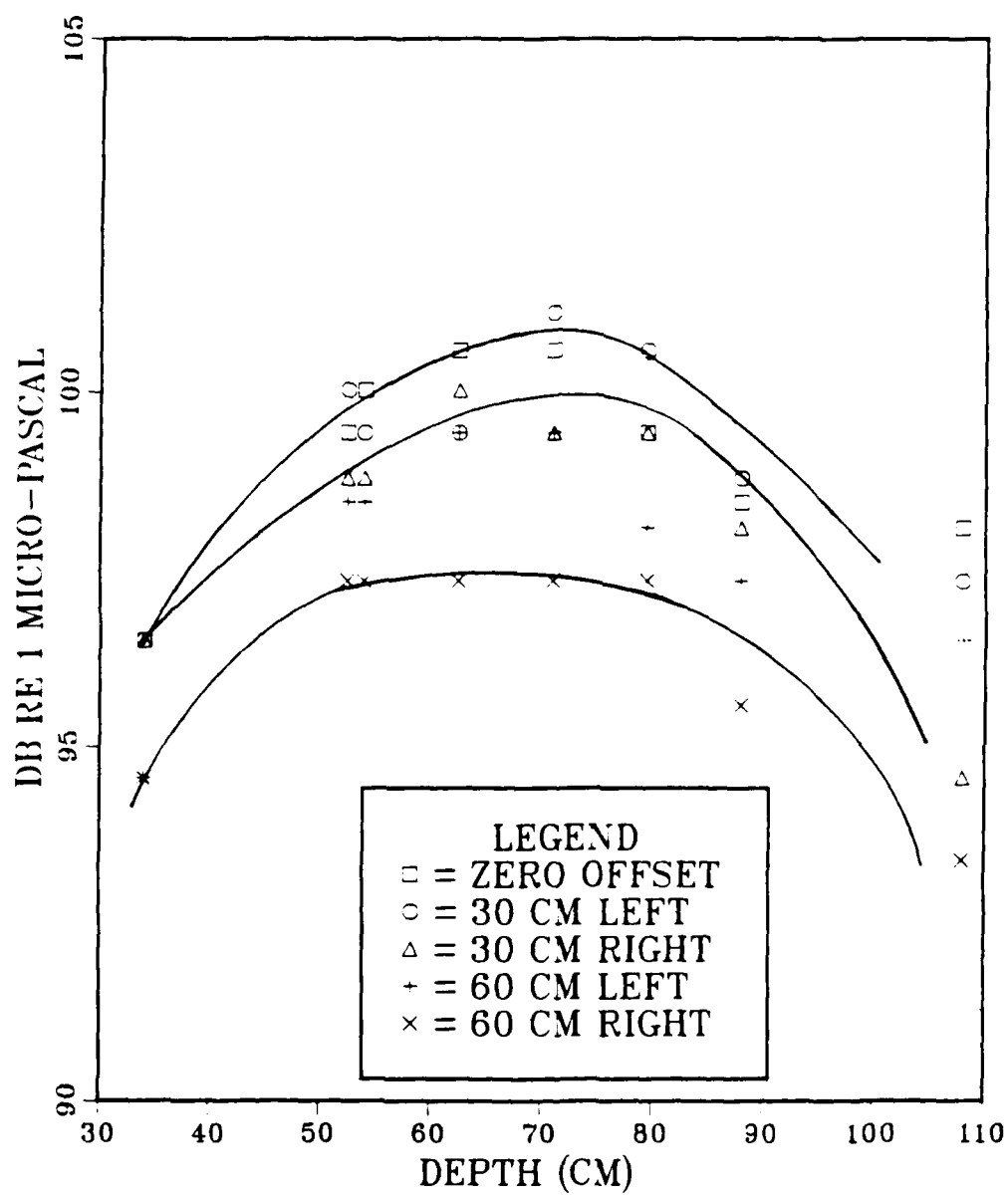


Figure 8. Sound Level at Target Site

## IV. RESULTS

### A. GENERAL

The results of the experiment are displayed graphically as target strength amplitude vs. depth in Figures 9 through 11 for the vertically suspended cylinder and in Figures 12 through 14 for the horizontally suspended cylinder. Target strength amplitude vs. horizontal offset is presented for the vertically suspended cylinder in Figures 15 through 17 and Figures 18 through 20 for the horizontally suspended cylinder. In general, the amplitude of target strength for the plastic cylinder was less than for the metal cylinder over all depths and positions. When data points from the same offset were compared over all depths, the target strength generally fell off at the extremes of upper and lower depths. This factor can be attributed to the effect of the reduced sound level at the target site (which was discussed in the previous section) and also to the reduced area of target presented to the source and receiver. The same trend is seen in the horizontal cylinder at varied depths.

When the data is presented with depth held constant and horizontal offset varied, the results are less clear-cut, although there is a general trend for the target strength to decrease at the extremes of off-center positions. The reduction in the amplitude can be attributed to the same factors that reduced target strength with respect to depth. There appears to be a pronounced effect from multipath signals off the sides of the tanks at the off-center positions which tended to enhance some signals. Additionally, as the horizontal cylinder was offset to  $\pm 60.0$  cm, the possibility that sound waves were striking the

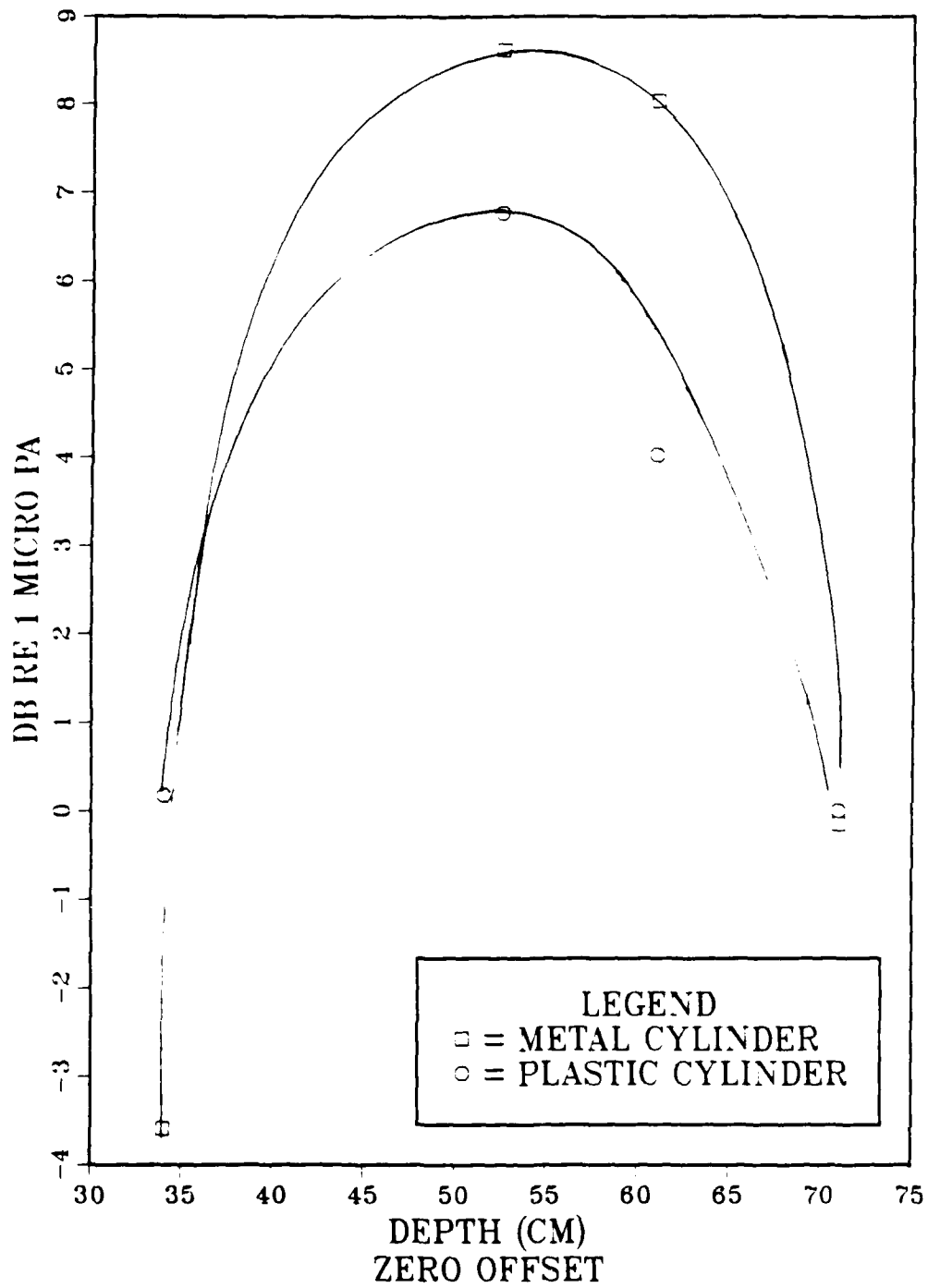


Figure 9. Vertical Cylinder Target Strength

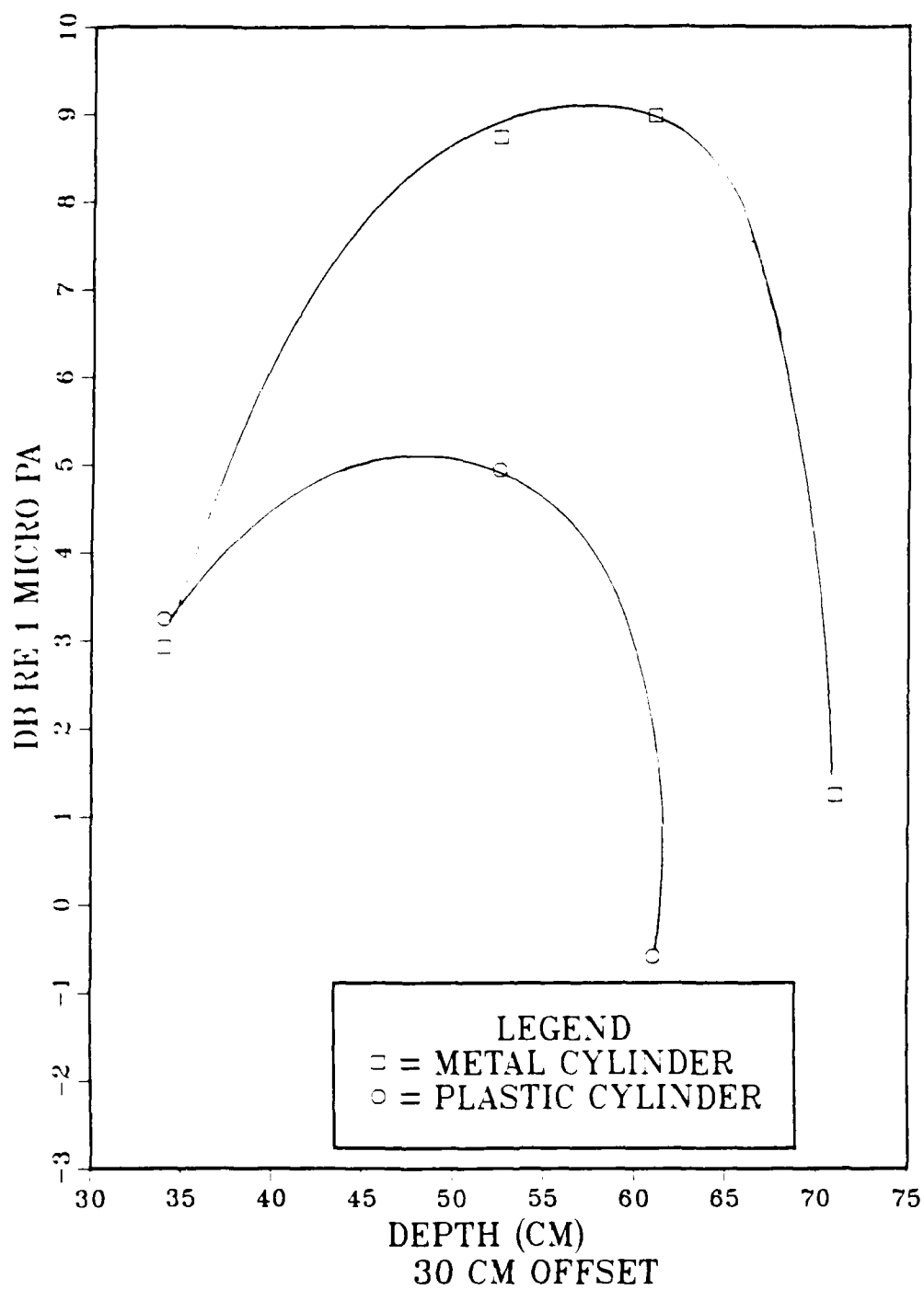


Figure 10. Vertical Cylinder Target Strength

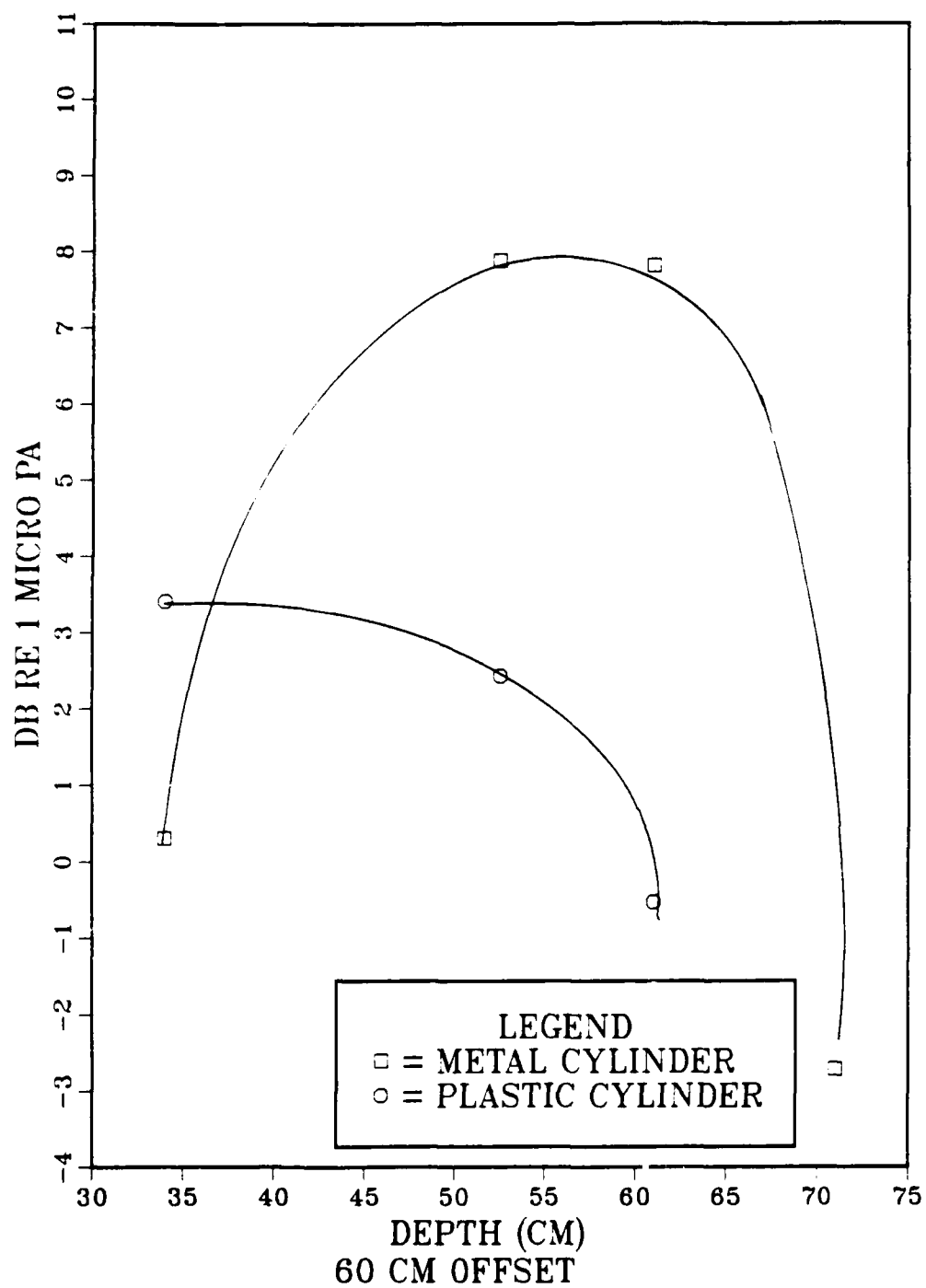


Figure 11. Vertical Cylinder Target Strength

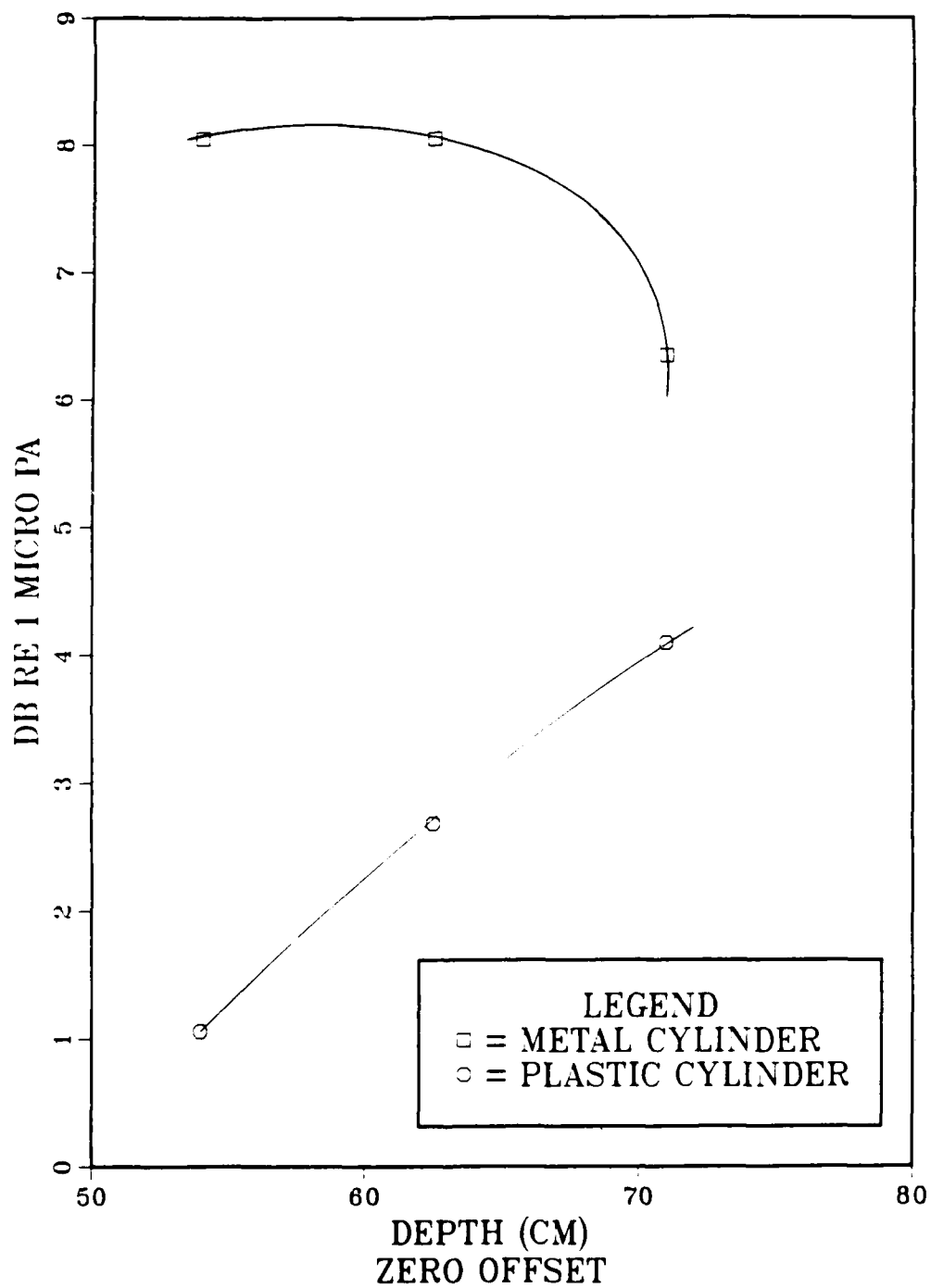


Figure 12. **Horizontal Cylinder Target Strength**

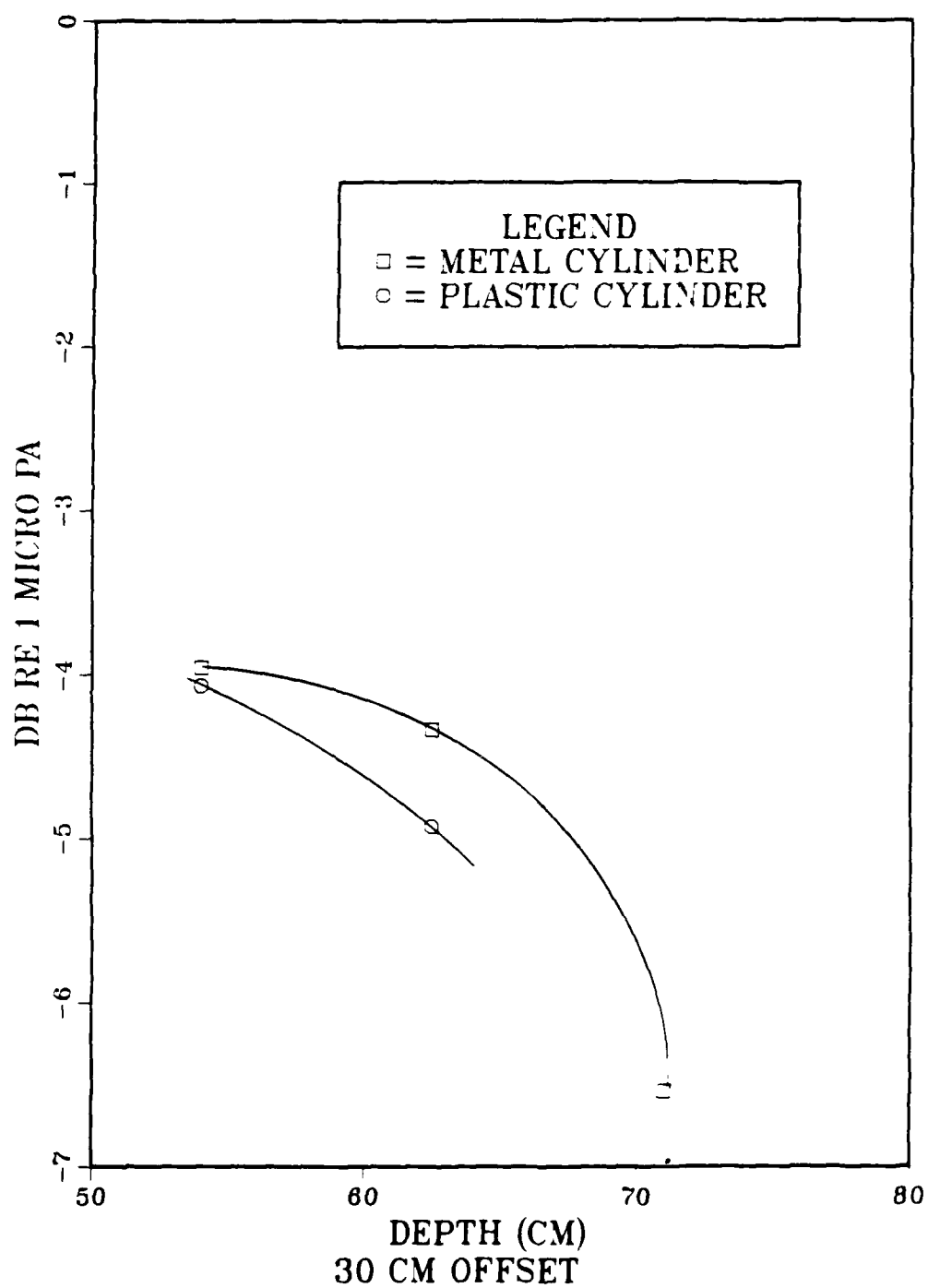


Figure 13. **Horizontal Cylinder Target Strength**

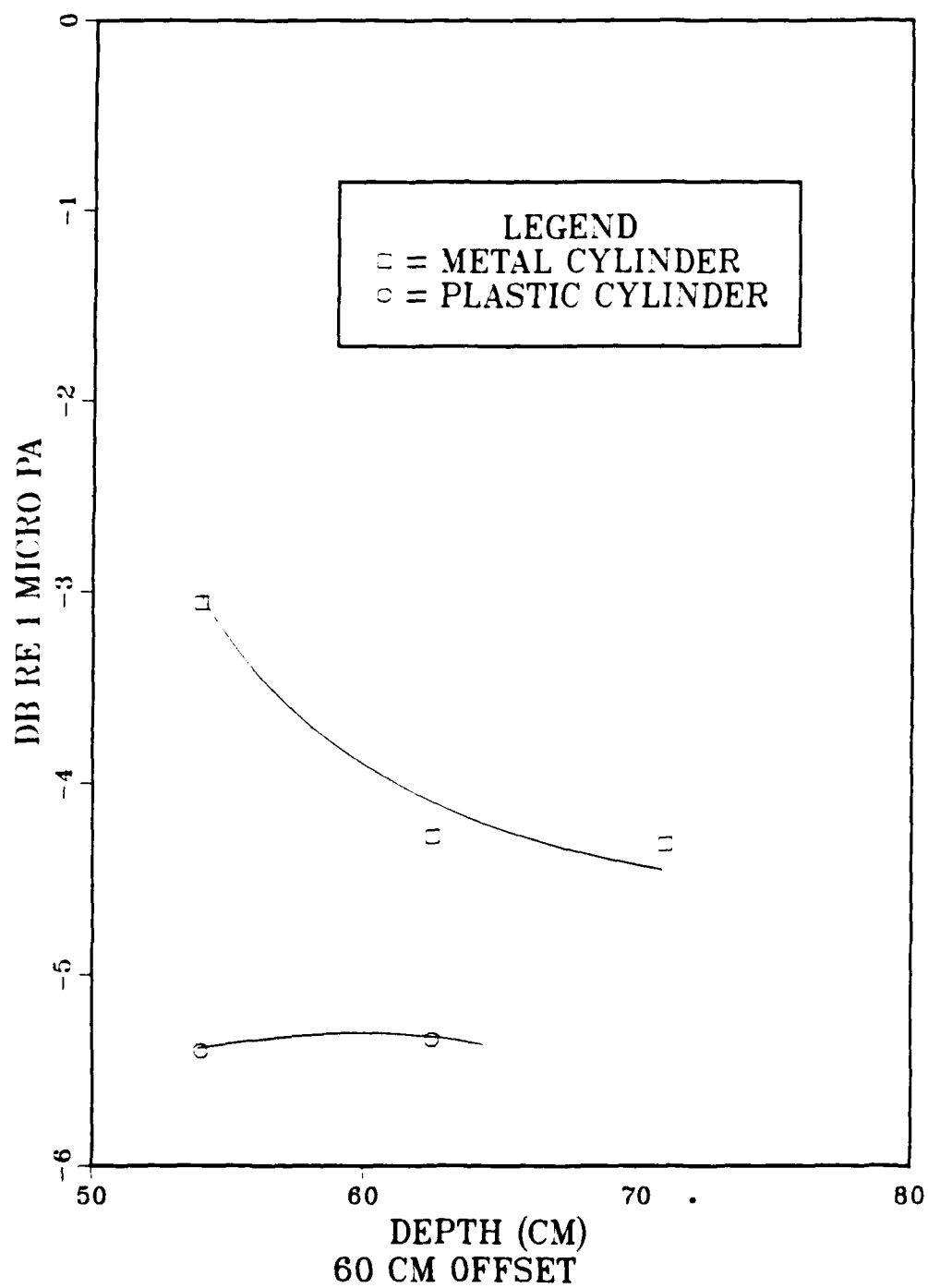


Figure 14. Horizontal Cylinder Target Strength



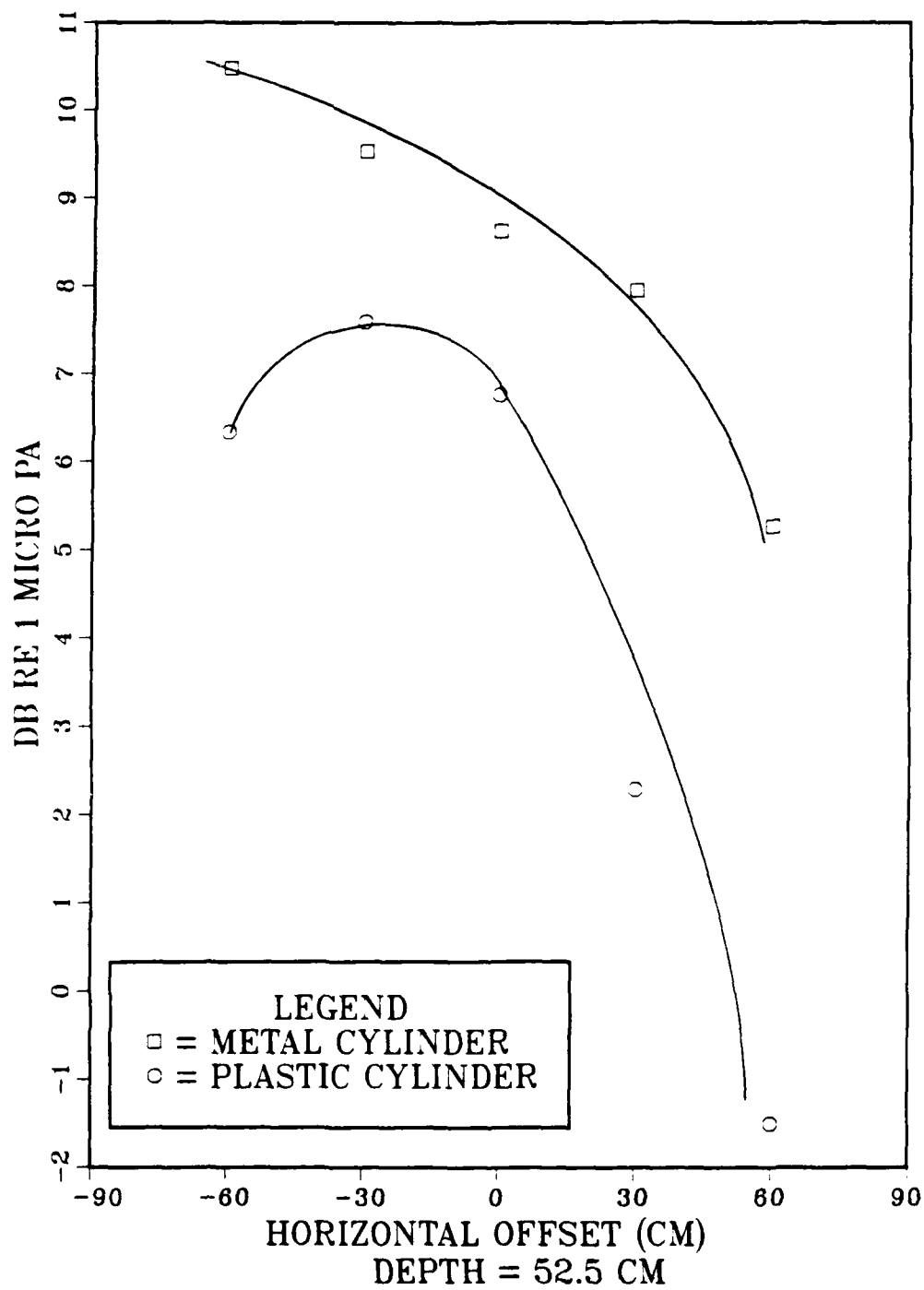


Figure 15. Vertical Cylinder Target Strength

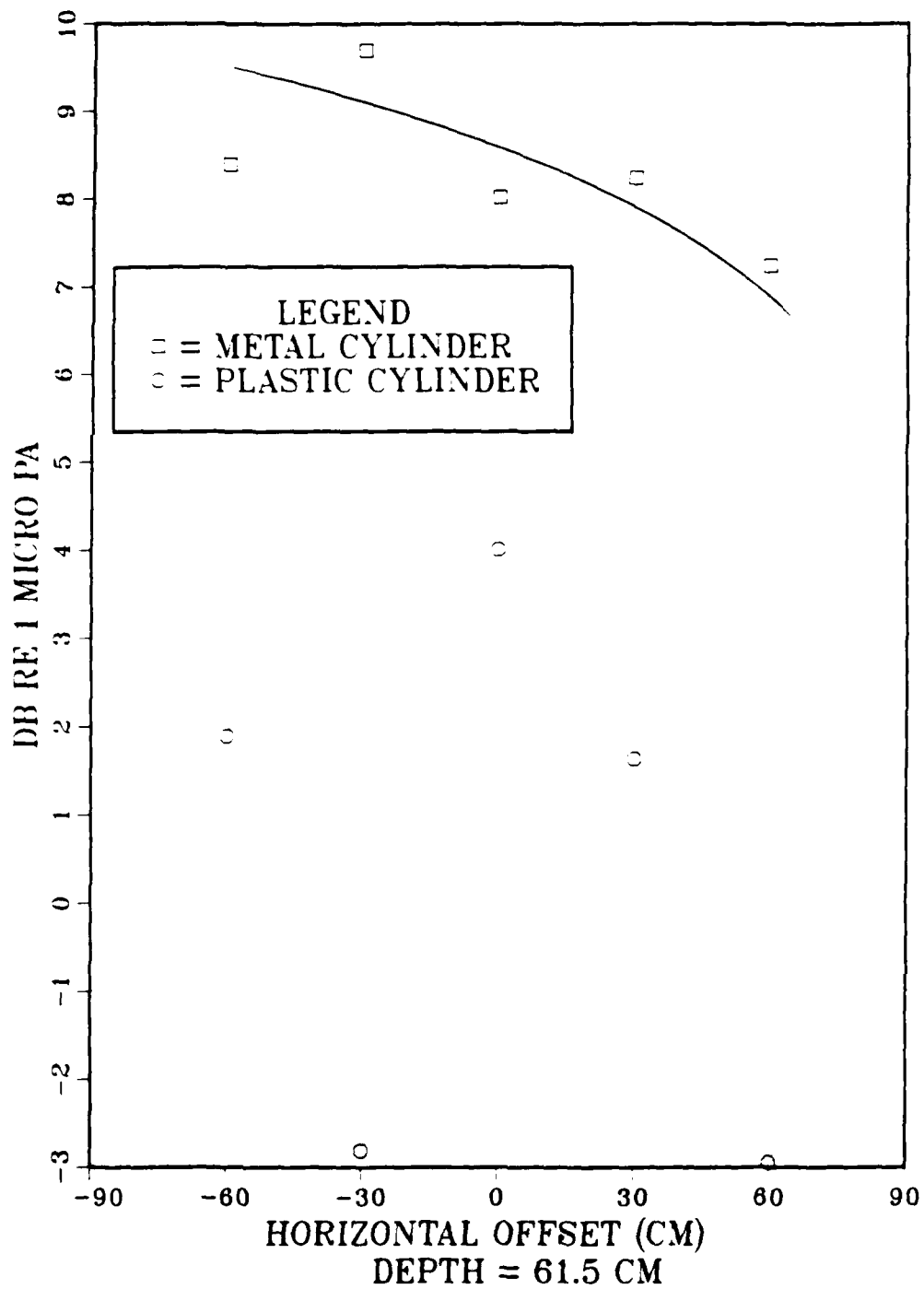


Figure 16. Vertical Cylinder Target Strength

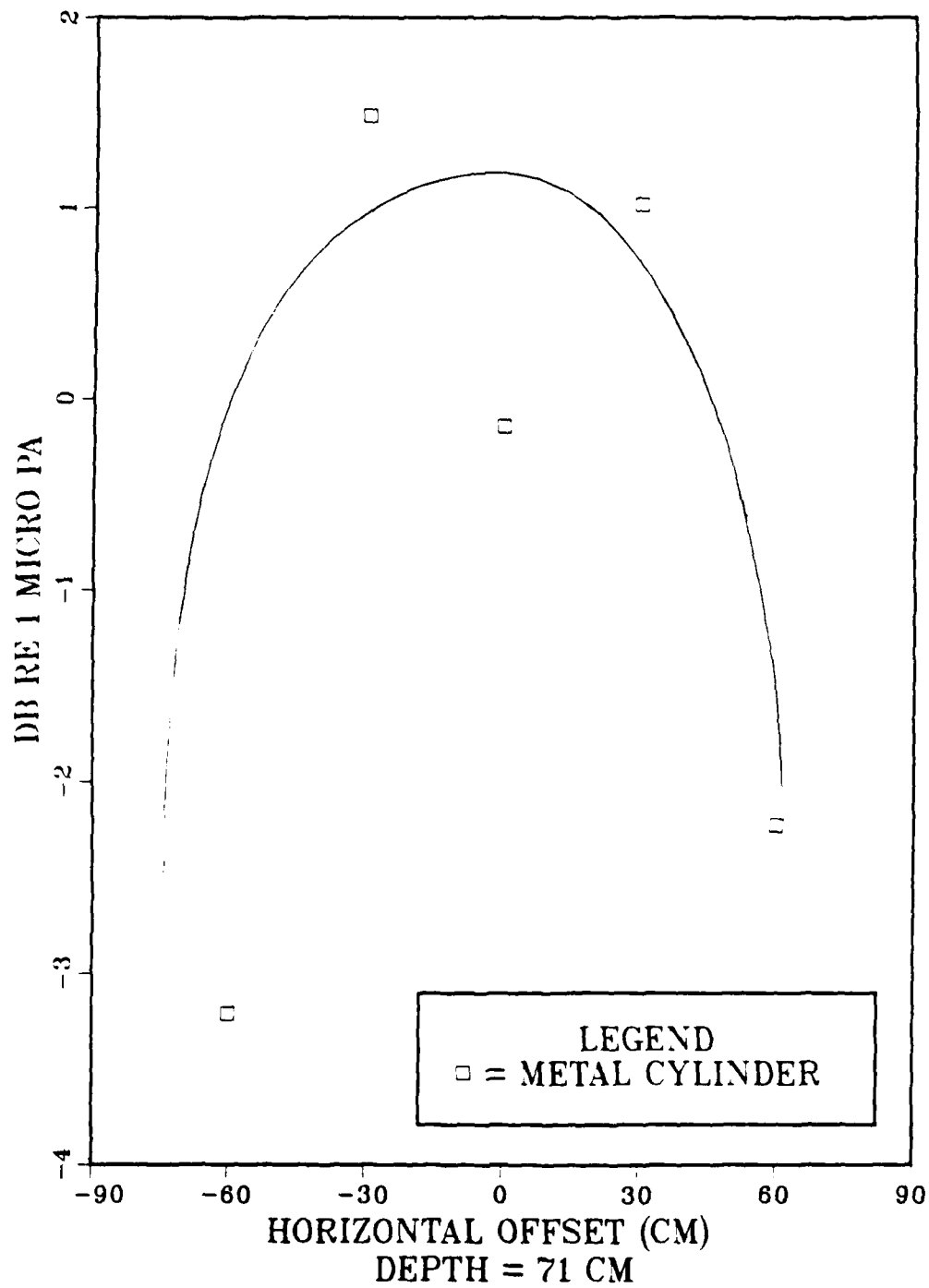


Figure 17. Vertical Cylinder Target Strength

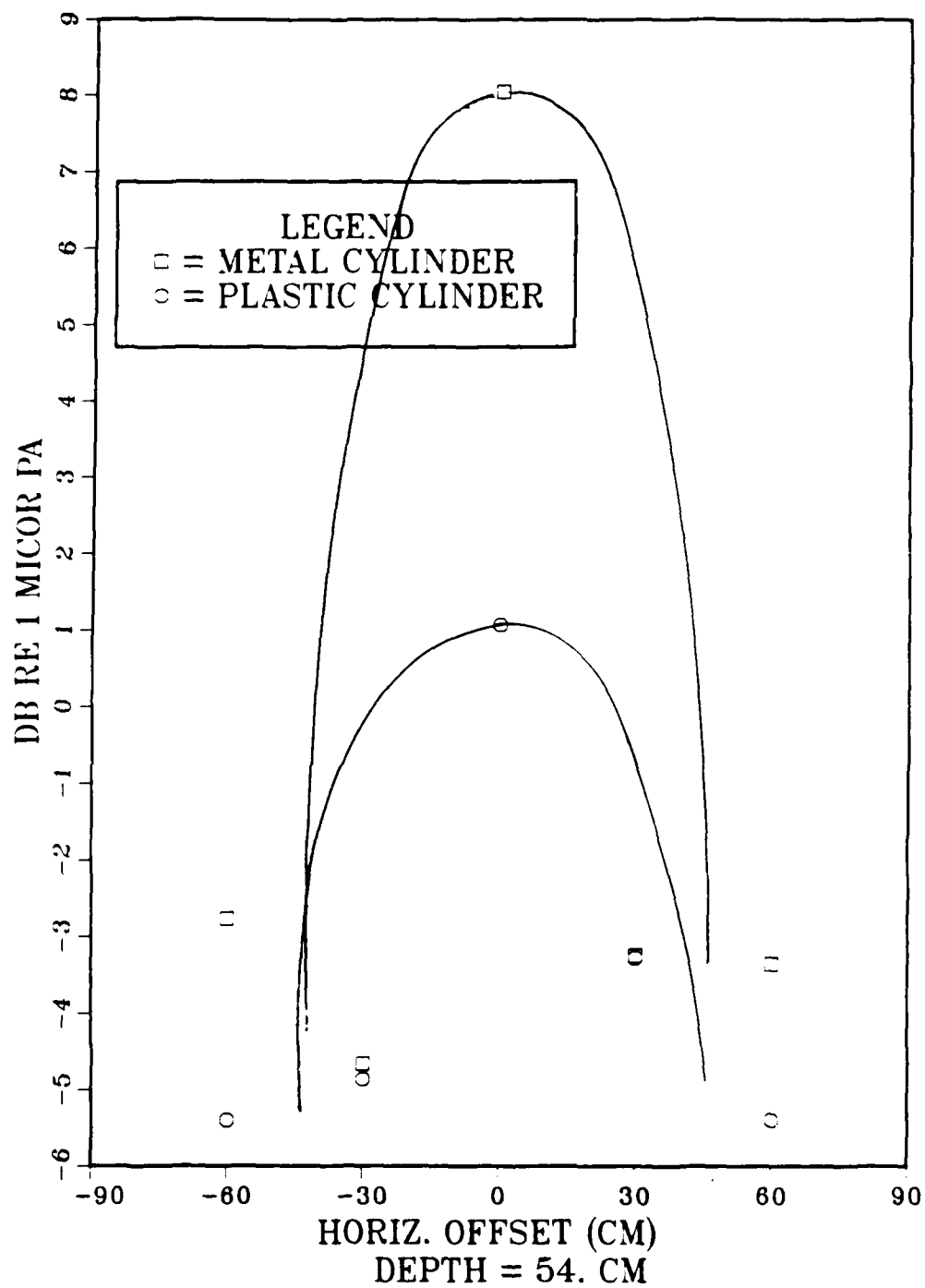


Figure 18. **Horizontal Cylinder Target Strength**

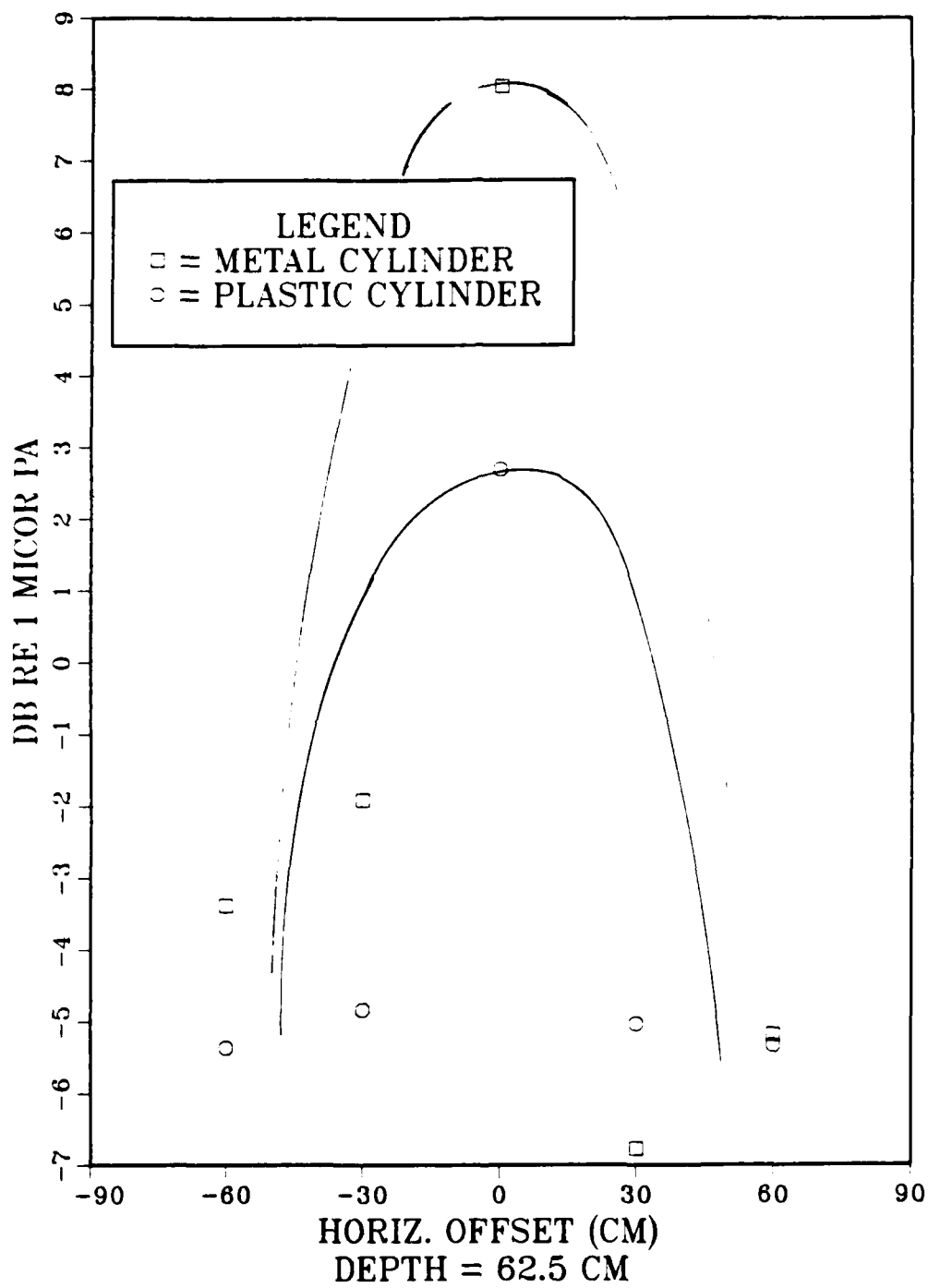


Figure 19. **Horizontal Cylinder Target Strength**

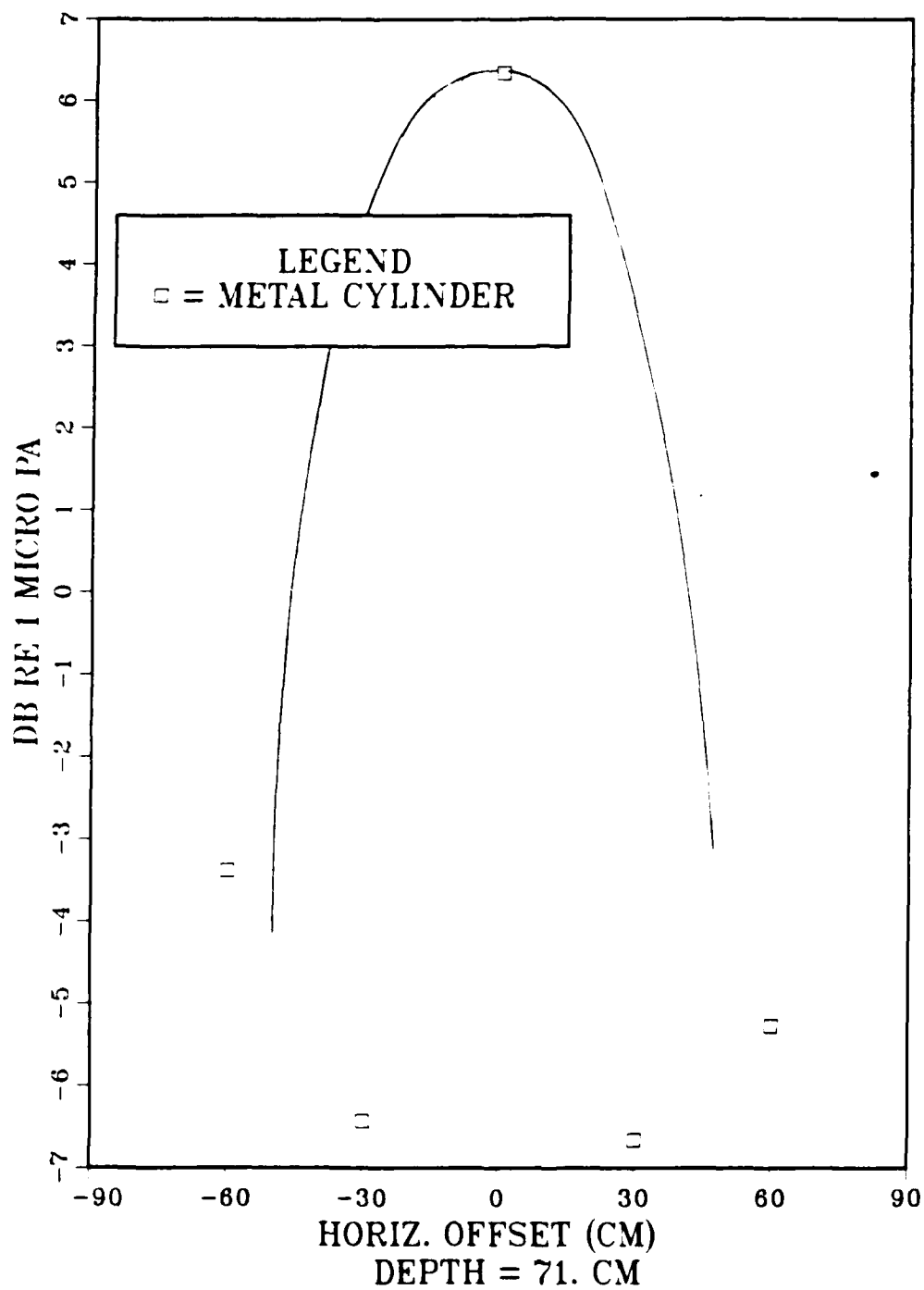


Figure 20. **Horizontal Cylinder Target Strength**

end and internal surfaces of the cylinder further complicated the analysis of the target strength. Stewart [Ref. 5] dealt with the problem of reduced target strength in his model by constructing envelopes of equal amplitude emanating from the receiver, each corresponding to a specified scattering strength, where targets with scattering strength above a given threshold would be detected while those of a lesser strength might or might not, depending on their location. The actual boundary from which a pulse would be detected is a function of power level, transmitter beam pattern, transmission loss, noise level, and receiver characteristics.

Identifying and categorizing cross-sections would therefore most likely occur on axis at a distance specified by a related envelope of detection.

#### **B. COMPARISON WITH ANALYTICALLY DERIVED TARGET STRENGTH ESTIMATES**

The target strength of a fully insonified finite cylinder was calculated using the method presented by Gaunard [Ref. 11]. The high-frequency approximation using the Fresnel Zone method leads to the expression:

$$TS = AL^2/2\lambda \quad (6)$$

where

A = radius of cylinder  
L = length of cylinder  
 $\lambda$  = wavelength of beam

This equation can only be used, however, if the separation between receiver and target is greater than the "Rayleigh distance," which equates to  $L^2/\lambda$ . In the case of this experiment, the Rayleigh distance is calculated to be 1850 cm, much greater than the conditions in the laboratory set-up. In his paper, Gaunaud advises:

If one is constrained to operate at small wavelengths, then one must be very far away from a finite length cylinder to be able to make far field observations of its returned echoes. Since this is hardly possible in the laboratory, one makes the measurements anyway, at smaller distances, with the understanding that this near field data cannot be compared to the far field results of the finite cylinder....It soon becomes clear that it must be compared to the far field result of the infinite cylinder.

The target strength of an infinite cylinder under spherical waves, still at large distances;  $R \gg A$  is found to be:

$$TS = 10 \log (A/4R) \quad (7)$$

where

R = the distance between receiver and target  
A = the cylinder radius

For this experiment, a representative  $R = 81.0$  cm and  $A = 8.5$  cm gives a target strength of -15.81 dB. This number does not correlate well with the experimental results; for this particular case, TS was found to be 8.61 dB for the metal cylinder and 6.75 dB for the plastic.



In all probability, distance between target and receiver were still too small to utilize this far-field approximation. In addition, this method cannot distinguish between rigid and soft targets and predicts cross-sections somewhere between the two extremes of behavior [Ref. 11].

### **C. LIMITATIONS DUE TO NOISE**

In performing the experiments in a finite body of water, the problem of surface-reflected noise from the side walls and free surface could not be ignored; the magnitude of these spurious returns was in some cases of equal strength to the poorest target returns and in some cases tended to mask the target from the observer. True target echoes could be distinguished from false by initiating a small amount of movement of the target relative to the receiver; the shift in time delay of the moving echo allowed for it to be identified as a "true" signal. Ensuring that the target and receiver were located in the geometric center of the tank would help provide separation between target and false echoes. Additionally, mechanically shielding the receiver and employing a directional source could have reduced the side-wall reflections.

### **D. CONCLUSIONS**

This work has presented a description of an experimental study of underwater acoustic returns from cylindrical targets, both metal and plastic, to determine whether target strength information can be used to identify object characteristics. The results showed that:

1. Target strength can be used to distinguish between the metal and plastic cylinders. However, other factors, such as position of the target relative to the transducer, reduce the amplitude of the return.
2. Multipath and side-wall echoes enhanced some returns when the target was near the surface or sides of the tank.

#### **E. RECOMMENDATIONS**

The following recommendations are made for future studies, based on the findings of this initial work:

1. Employ a narrow-beam transducer and initially insonify target on axis only to reduce effects from multipath returns.
2. Insonify a narrow, very long cylinder at greater distances if data is to be compared to mathematical equations; this should also reduce the effects of sound reflecting off the inside edges of the open-ended cylinder.
3. Refine the basic sonar equation by including:
  - a. detection threshold, which accounts for signal-to-noise ratio and the probability of the target being identified in ambient noise; and
  - b. directivity index, which accounts for the probability of a directional sonar picking up the echo in its field.

## LIST OF REFERENCES

1. Bane, J., "The Evolutionary Development of the Military Autonomous Underwater Vehicle," 5th Symposium on Unmanned Untethered Submersible Technology (UUST), p. 60-88, June 1987.
2. Robinson, R., "National Defense Applications of Autonomous Underwater Vehicles," *IEEE J. of Oceanic Eng.*, v. OE-11, pp. 462-467, November 1986.
3. "Acoustic Telemetry Links and High Resolution Sonar," 3rd Symp. on UUST, pp. 185-7, June 1983.
4. Mobile Robot Laboratory, Carnegie Mellon University, Report CMV-R1-MRL 86-1, *Autonomous Mobile Robots Annual Report 1985*.
5. Stewart, W. Kenneth, "A Non-Deterministic Approach to 3-D Modeling Underwater," 5th Symposium on UUST, pp. 283-307, June 1987.
6. Mazel, C. H., "Inspection of Surfaces by Side-Scan Sonar," Remotely Operated Vehicles, pp. 24-28, 1984.
7. Glynn, James M., "Considerations for Acquisition and Processing of Side-Scan Sonar Data By an Autonomous Submersible," 4th Symp. UUST, pp. 109-113, June 1985.
8. Blidberg, D. Richard, and Chappell, Steven G., "Guidance and Control Architecture for the EAVE Vehicle," *IEEE J. of Oceanic Eng.*, v. OE-11, No. 4, pp. 449-461, October 1986.
9. Russell, George T., and Lane, David M., "A Knowledge-Based System Framework for Environmental Perception in a Subsea Robotics Context," *IEEE J. of Oceanic Eng.*, v. OE-11, No. 3, pp. 401-412, July 1986.
10. Kinsler, Lawrence E., Frey, Austin, Coppins, Alan B., and Sanders, James V., *Fundamentals of Acoustics*, 3rd ed., John Wiley & Sons, Inc., 1982.
11. Gaunaurd, Guillermo C., "Sonar Cross Sections of Bodies Partially Insonified by Finite Sound Beams," *IEEE J. of Oceanic Eng.*, v. OE-10, No. 3, July 1985, pp. 213-230.

# **INITIAL DISTRIBUTION LIST**

	<u>No. Copies</u>
1. Defense Technical Information Center Cameron Station Alexandria, VA 22304-6145	2
2. Library, Code 0142 Naval Postgraduate School Monterey, CA 93943-5002	2
3. Chairman, Code 69Hy Mechanical Engineering Department Naval Postgraduate School Monterey, CA 93943-5000	5
4. Professor D. L. Smith, Code 69Sm Mechanical Engineering Department Naval Postgraduate School Monterey, CA 93943-5000	1
5. Professor R. McGhee, Code 52Mz Computer Science Department Naval Postgraduate School Monterey, CA 93943-5000	1
6. Professor R. Christi, Code 62Cx Electrical and Computer Engineering Department Naval Postgraduate School Monterey, CA 93943-5000	1
7. Dr. G. Dobeck, Code 4210 Head, Navigation and Guidance NCSC Panama City, FL 32407-5000	1
8. Russ Werneth, Code u25 Naval Surface Weapons Center White Oak, MD 20910	1

9. Paul Heckman, Code 943 1  
Head, Undersea AI & Robotics Branch  
Naval Ocean System Center  
San Diego, CA 92152
10. Dr. D. Milne, Code 1563 1  
DTNSRDC, Carderock  
Bethesda, MD 20084-5000
11. RADM G. Curtis, USW PMS-350 1  
Naval Sea Systems Command  
Washington, DC 20362-5101
12. LT Rella L. Lyman, Jr., USN Code 90G 1  
Naval Sea Systems Command  
Washington, DC 20362-5101
13. Distinguished Professor G. Thaler, Code 62Tr 1  
Electrical and Computer Engineering Department  
Naval Postgraduate School  
Monterey, CA 93943-5004

**DAT  
FILM  
8**